

Chapter 5

Functional Nanoscale Devices

Herb Goronkin, Paul von Allmen, Raymond K. Tsui, and Theodore X. Zhu
Motorola

INTRODUCTION

The recent emergence of fabrication tools and techniques capable of constructing structures with dimensions ranging from 0.1 to 50 nm (see Fig. 5.1) has opened up numerous possibilities for investigating new devices in a size domain heretofore inaccessible to experimental researchers. The WTEC nanotechnology panel reviewed research in the United States, Japan, Taiwan, and Europe to find that there is considerable nanoscience and technology activity in university, industrial, and government laboratories around the world. The insight gained from this survey suggests areas of strength and areas of possible improvement in the field.

There is intense study around the world to determine the exact point in dimensional scaling where it becomes either physically unfeasible or financially impractical to continue the trend towards reducing the size while increasing the complexity of silicon chips. In some of the same laboratories where research activities on Si are decreasing, research activities on single-electron devices (SEDs) are increasing. Although there are myriad questions involving electrical contacts, interconnections, reliability, and the like, one of the fundamental issues in the miniaturization/complexity debate concerns the Si MOSFET itself when the gate length is reduced to less than 50 nm. Does it behave like a long gate device or does the output conductance increase to impractical levels due to short-channel effects? Based on the WTEC panel's survey, most of the activities examining these questions are taking place in Japanese industrial laboratories.

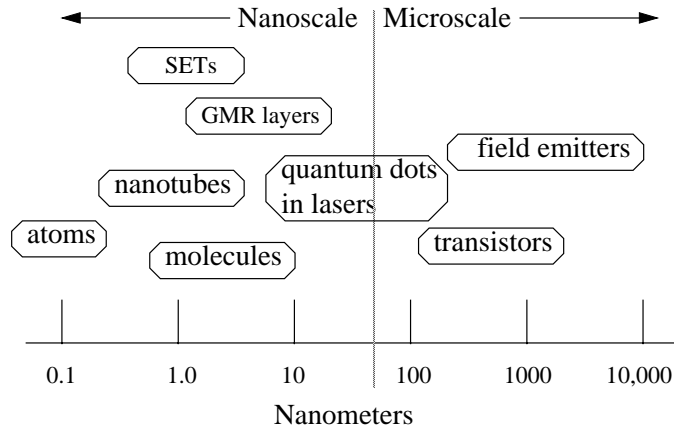


Figure 5.1. Functional device scales.

While the signature current-voltage (I-V) characteristics provide a common basis for comparison of device performance, there are significant variations in the fabrication methods and device structures being considered by the different labs in the countries the panel surveyed that have significant SED activity. The range of research in the surveyed laboratories spans electrical measurements from millikelvin to room temperature and from discrete electronic elements to integrated single-electron transistors (SETs). Materials that are used to form the active single-electron element range from charge clusters that are shaped by electric fields in a two-dimensional electron gas to metallic colloids to single oligomers. Progress in the field is hindered by architectures based on conventional circuit approaches that fail to take sufficient advantage of the unique properties of single-charge electronics to achieve significant impact in future high density applications. Most research in SED technology is fundamental and is distributed among universities funded by government agencies. A smaller body of application-directed research exists in industrial laboratories; these are mostly in Japan.

The field of magnetics has experienced increasing attention since giant magnetoresistance (GMR) in multilayered structures was discovered in 1988. In these structures ferromagnetic layers are quantum mechanically coupled across a 1-3 nm nonmagnetic metallic layer. GMR structures are under intense study for applications in hard disk heads, random access memory (RAM), and sensors. Several laboratories are investigating the physics of the transition of these layers, which are quantum mechanically confined in one dimension, to layered filaments in which there are one- and two-dimensional confinements. There are numerous experimental process approaches under consideration in fabricating GMR structures, including the following:

- magnetron or ion beam sputter deposition
- epitaxy for layered structures
- rubber stamping of nanoscale wire-like patterns
- electroplating into nanoscale pores in polymer membranes

In RAM applications, a high ratio of magnetoresistance combined with a small coercive switching field is key to density, speed, and low power. These features are also achieved in magnetic tunnel junctions in which the ferromagnetic layers are quantum mechanically coupled through a thin dielectric layer. Although research in nanoscale magnetics is underway internationally, most of the activities on the practical applications mentioned above are in the United States.

Optical devices have already benefited from incorporation of nanostructured materials: commercially available semiconductor lasers incorporate active regions comprised of quantum wells, the presence of which modifies the electronic density of states and the localization of electrons and holes, resulting in more efficient laser operation. Extrapolating from those results, even greater improvements are predicted for lasers utilizing either quantum wire or quantum dot active layers. Recent advances in the “self-assembled” formation of quantum dot structures have stimulated progress in the fabrication and characterization of quantum dot lasers in Japan, Europe, and the United States.

In late 1991, the first synthesis and characterization of carbon nanotubes were reported. The novel material contained a wide variety of multiwalled nanotubes (MWNT) containing 2 to 50 concentric cylindrical graphene sheets with a diameter of a few nm and a length of up to 1 μm . The material was produced at the negative electrode of an arc discharge and appeared to be mixed with a large amount of other forms of carbon. This initial work led many groups throughout the world to produce and purify nanotubes. The theoretical study of their electronic structure followed in the next year. Soon it became clear that nanotubes have unique electronic and mechanical properties that are expected to lead to ground-breaking industrial applications. Some of the progress made in this respect over recent years is summarized later in this chapter.

SINGLE-CHARGE ELECTRONICS

Even though the study of single-electron charging effects with granular metallic systems dates back to the 1950s, it was the research of Likharev and coworkers almost 10 years ago that laid much of the groundwork for understanding single-charge transport in nanoscale tunnel junctions (Likharev 1988; Averin and Likharev 1991, Chap. 6). The concept was developed of a Coulomb gap that can be exploited to control the transfer of

single charges. Since then, many research groups have made use of the Coulomb blockade effect to develop SED technology. Figures 5.2 through 5.11 show some of the myriad approaches to developing SEDs and representative laboratories pursuing the various SED concepts. Some of the more recent results are discussed below.

The group at Hitachi Europe uses a side-gated constriction in a delta-doped GaAs structure to fabricate a magnetic tunnel junction device in which a series of small islands separated by tunnel barriers are formed (Nakazato et al. 1992) (see, for example, Fig. 5.2). At ~ 2 K, the Coulomb gap voltage oscillates as a function of the side-gate voltage. Using the MTJ device as a building block, both memory and logic (inverter, NOR) functions have been demonstrated (Nakazato 1996, 65). The fabrication procedure makes use of standard semiconductor processing techniques and does not rely on lithography to define the nanoscale islands, since these are created by disorder in the delta-doped layer.

Other groups have utilized fine-line lithography to fabricate SEDs. At IBM, a flash memory SED was demonstrated by fabricating a sub-50 nm Si quantum dot (QD) on top of a MOSFET channel using a silicon-on-insulator (SOI) substrate, with the QD acting as a floating gate (Wesler et al. 1997). Single-electron charging was observed up to 90 K, while large threshold voltage shifts of up to 0.75 V were measured at 290 K. The University of Minnesota and Fujitsu have also reported similar structures (Guo et al. 1977; Nakajima et al. 1997). To overcome the lithography limitation on the QD size, the Toshiba group used a Si edge quantum wire approach (Ohata and Toriumi 1996). An inversion layer was formed at the 15 nm high Si sidewall of a SOI structure by growing a gate oxide and depositing a poly-Si gate there. Conductance oscillations were clearly seen at 4.2 K in this edge-channel MOSFET (Fig. 5.3). More recently, the Toshiba group has reverted back to a more planar device configuration, with a 50 nm wide Si quantum wire defined by e-beam lithography and oxidation of the surrounding SiO_2 (Koga et al. 1997, 79).

One method to form semiconductor QDs without depending on fine-line lithography is to make use of the self-organizing nature inherent in the Stranski-Krastanow thin film growth mode. In the initial stages of the heteroepitaxial growth of lattice-mismatched materials, strain-induced coherent relaxation occurs and dislocation-free islands are formed that are in the tens of nanometers range in size. There has been considerable research in these self-organized quantum dots (SOQDs) in the past few years, though much of the work has been of a fundamental nature (see, for example, Petroff and Demmester 1995; Nötzel 1996). More recently, the University of Tokyo has proposed the embedding of InAs SOQDs in AlGaAs/GaAs heterojunction field effect transistors (HFETs) to form a flash-memory SED (Sakaki et al. 1995).

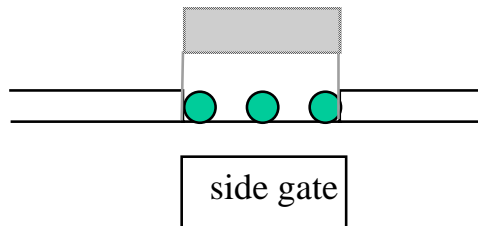


Figure 5.2. Metal colloids, self-assembled monolayer (SAM) coatings, polysilicon, quantum dots embedded in SiO₂ (Hitachi, IBM, RIKEN, NTT, ETL, University of Lund).

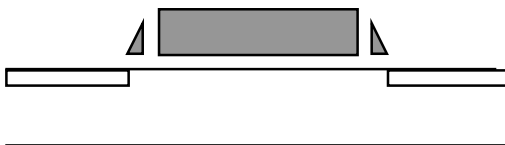


Figure 5.3. Sidewall extensions of MOSFET gate (Toshiba).

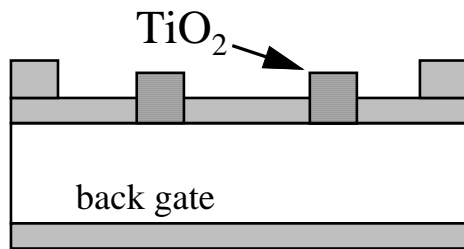


Figure 5.4. Oxidation of metal or semiconductor with scanning tunneling microscope (STM) tip (ETL).

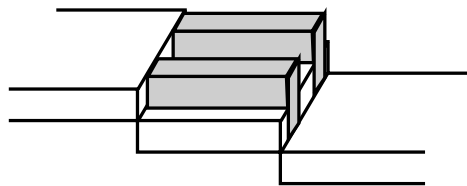


Figure 5.5. STM probe oxidation of metal on vicinal substrate steps (ETL).

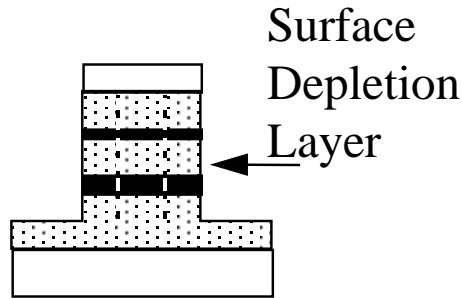


Figure 5.6. Double barrier tunnel diode structure (Max-Planck-Institut, Stuttgart; NTT).

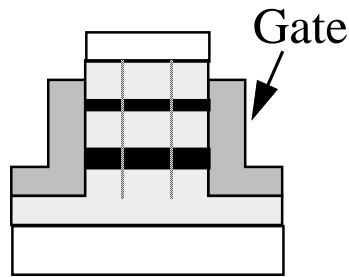


Figure 5.7. Gated double barrier tunnel diode structure (Max-Planck-Institut, Stuttgart; NTT; Purdue University).

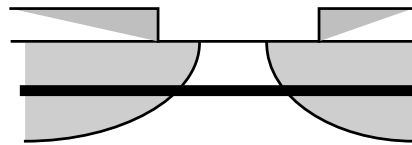


Figure 5.8. Depletion layer control of 2DEG area (Hitachi, University of Glasgow, University of Tokyo).

This concept was further demonstrated by the Sony group, which reported observing threshold voltage shifts at 300 K (Taira et al. 1997, 53). Fujitsu has also proposed the use of InGaAs QDs in a similar manner (Futatsugi et al. 1997, 46). The one difference in this case is that the QDs are formed at the bottom of tetrahedral-shaped recesses formed by substrate patterning. Since SOQDs form in a somewhat random manner on a planar surface, this approach provides positioning control.

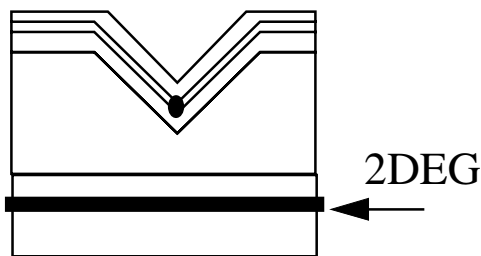


Figure 5.9. Tetrahedral shaped recess, TSR (Fujitsu).



Figure 5.10. Double barrier metallic SET patterned by e-beam (NEC).

Of course, QDs can be formed with materials other than semiconductors. In fact, some of the earliest work in single-electron charging was done with metallic tunnel junctions. With modern fabrication tools and techniques, some groups have investigated the formation of nanoscale Au particles between metallic contacts. The University of Cambridge group used focused ion beam deposition to place Au dots between electrodes spaced 30 - 40 nm apart (Woodham and Ahmed 1997, 73). At Lund University in Sweden, atomic force microscopy (AFM) is utilized to move a 50 nm Au particle in between contacts formed by e-beam lithography (Carlsson et al. 1997, 128). Researchers observed conductance plateaus stable for several minutes at 300 K. The group at Cambridge University/Hitachi Europe used a colloidal process to form a chain of insulated Au particles between source, drain, and gate electrodes (Tsukagoshi et al. 1997, 67). At 4.2 K, the chain exhibited a Coulomb staircase and periodic conduction oscillations in I-V measurements.

For a very different approach, a molecular embodiment of a QD-based system can be realized by connecting a single molecule between metallic contacts. At Yale University a single molecule of benzene-1,4-dithiol was self-assembled from solution onto two electrodes of a mechanically controllable break junction (Fig. 5.11, left) (Reed et al. 1997). The spacing between the electrodes is ~ 0.8 nm, and I-V measurements at room temperature showed a gap ~ 0.7 V wide, which is attributed to a Coulomb gap. The Delft University of Technology in the Netherlands is also working on transport through oligomers (Fig. 5.11, right).

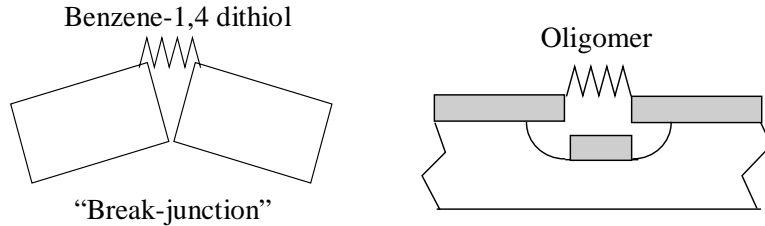


Figure 5.11. A single molecule connecting metallic contacts (Yale University, University of South Carolina, Delft University, Karlsruhe University).

Concerning the architecture in which SEDs are utilized, a number of approaches have been proposed. One of the more novel ideas is that of quantum cellular automata (QCA), based on some earlier work at Texas Instruments and developed at the University of Notre Dame (Lent et al. 1993; Tougaw and Lent 1994). The basic QCA cell is made up of a group of capacitively coupled QDs. Each cell holds two electrons, resulting in two polarization configurations that can represent the logic “0” and “1” states, and each cell interacts via Coulombic forces with neighboring cells. An array of cells can then be used to transmit binary information, which eliminates the need for physical interconnects between devices and represents a paradigm shift for ultralarge-scale integration (ULSI). Basic Boolean operations (AND, OR, etc.) can be implemented using QCA, and more complex functions have been simulated. Most recently, the Notre Dame group has demonstrated a nonlinear, bistable response of a QCA cell, albeit at a very low temperature of less than 20 mK (Snider et al. 1997, 233).

The QCA approach is not without its challenges (and critics). Circuit fabrication will be difficult because stringent control in QD positioning is required. Others have pointed out that bistability is only a necessary but not sufficient condition for the operation of Boolean logic circuits, because isolation is needed between the input and output, while background charge fluctuations will hamper logic implementation (Roychowdhury et al. 1996; Barker et al. 1997, 233). Thus, there is also considerable research in the use of SEDs with more conventional architectures. The group at Hitachi Europe uses its MTJ devices in binary decision diagram logic that is commonly used in large-scale integrated (LSI) circuits (Tsukagoshi et al. 1997, 67). The Toshiba group is combining its SED with a MOSFET to compensate for the lack of gain in the former, as are, presumably, other groups working on QD-based flash memory SEDs (Koga et al. 1997, 79). Tables 5.1 and 5.2 summarize some of these approaches.

TABLE 5.1. SET Architectures

Flash Memory	Digital Logic	Cellular Automata	Neural Networks
Hitachi	Hitachi (binary decision diagram logic)	Notre Dame Hitachi	Delft U. Technology
IBM	Hokkaido University		
Toshiba			

TABLE 5.2. Quantum Dot Flash Memory

	Hitachi	Minnesota	Fujitsu	IBM	Sony
Material	Poly-Si	SOI	SOI	SOI	GaAs
QD Material	Poly-Si	Poly-Si	Poly-Si	Poly-Si	InAs
QD Fab Method	E-beam / etch	E-beam / etch	E-beam / etch	E-beam / etch	Epitaxial self-assembly
QD Size (nm)	10 (estim.)	7 x 7 x 2 h	30 x 20 x 25 h	30 x 20 x 8 h	25 x 4 h
2V _{th} (V)	0.5 - 1.0	0.055	0.1	0.75	0.45
Write/ Erase	15 V / 10 V	> 4 V	4 V	3 V	> 1 V
Retention	1 - 24 h	10 sec.		> 1 wk	10 sec.
Circuits	128 Mb LSI				

In summary, while significant progress has been made in nanofabrication techniques, the field of single-charge electronics is still limited in scope by the lack of a suitable architecture that fully utilizes the unique aspects of single-electron charging. Current approaches require many SED elements to achieve conventional functions such as adders, exclusive NORs, etc. Simulations of such circuits predict slow operating speed. The field seems to be stuck on applying conventional electronics to SEDs. Either a new architecture will be discovered or SEDs may find a niche home in those applications where measurements of single charges are needed.

For the fabrication of nanoscale electronic devices, the self-organizing technique appears to be the most promising. The field of self-organized semiconductor QDs is quite active, but aside from optical emitters, very few practical electronic functions have been proposed. Of those, the single-electron flash memory is attracting attention, but there has been no serious proposal as to how the device could operate under normal integrated circuit performance conditions and reliability specifications. Using the SED as a floating gate to a MOSFET has the same kinds of problems as applying conventional approaches to SED architectures; until someone comes up with a better idea, the future of these approaches remains to be determined.

NANOMAGNETICS

The discovery in 1988 of GMR in structures of alternating magnetic and nonmagnetic thin layers (Baibich et al. 1988) was the accumulation of several decades of intensive research in thin film magnetism (Shinjo and Takada 1987) and improvements in epitaxial growth techniques developed mainly in semiconductor materials. Not surprisingly, the first GMR structure was fabricated using molecular beam epitaxy (Baibich et al. 1988). The high quality magnetic and nonmagnetic metallic films provide electrons with a mean free path exceeding 100 Å; on the other hand, the epitaxial growth allows for each constituent layer of the structure to be as thin as a few atomic layers. The greatly enhanced spin-dependent scattering in these multilayered structures provides magnetoresistance changes as high as 50%. Table 5.3 shows some of the institutions involved in GMR research and development, based on various publications, patents, and WTEC visits.

Two subsequent major developments from IBM enabled the application of GMR materials to hard disk heads, RAM, and sensors. The first development was the demonstration of equally good or better GMR materials using high throughput and production-worthy magnetron sputtering systems (Parkin et al. 1990). The other development was the invention of magnetically soft spin-valve structures, which allow low field and low power operation (Dieny et al. 1991a; Dieny et al. 1991b).

TABLE 5.3. Giant Magnetoresistance Activities

Memory:	MRAM	HD Heads	Structures / Physics / Materials
• Fujitsu	[green square]	[green square]	• IMEC
• Hitachi	[green square]	[green square]	• L'Ecole Polytechnique Lausanne
• Honeywell	[green square]		• IBM Zurich
• IBM	[green square]	[green square]	• Tohoku University
• Motorola	[green square]		• Nagoya University
• Matsushita	[green square]	[green square]	• NIST
• Mitsubishi	[green square]	[green square]	• UC Santa Barbara
• Philips		[green square]	• UC San Diego
• Samsung	[green square]		• Carnegie Mellon
• Toshiba	[green square]	[green square]	• Princeton
• Seagate		[green square]	
• Siemens	[green square]		
• Sony		[green square]	

*Based on publications, patents or visits.

Industrial R&D efforts on GMR materials initially focused on high density read heads. The major U.S. players are IBM, Seagate, Quantum, ReadRite, and Applied Magnetics. In Japan, all the semiconductor companies are involved, in addition to strong magnetic media powerhouses such as TDK and Yamaha. Korea's Samsung is also actively involved in the GMR race. In Europe, Thomson CSF, Philips, and Siemens seem to have fallen behind. All in all, IBM is in a commanding position to reap the benefits of the GMR phenomenon. In November 1997, it announced the volume production of the first generation of GMR read heads.

In 1995, a different class of high magnetoresistive materials was discovered in which the nonmagnetic layer separating the two ferromagnetic layers is made with an ultrathin insulating material, such as an aluminum oxide layer $< 20 \text{ \AA}$ thick (Miyazaki and Tezuka 1995; Moodera et al. 1995). With the switching of magnetization of the two magnetic layers between parallel and antiparallel states, the differences in the tunneling coefficient of the junction and thus the magnetoresistance ratio have been demonstrated to be more than 25%. A distinctive feature of this MTJ class of materials is its high impedance ($> 100 \text{ k}\Omega\text{-}\mu\text{m}^2$), which allows for large signal outputs.

The gradual improvement of GMR and MTJ materials have made them attractive for nonvolatile magnetic random access memory (MRAM) applications. The potential to make MRAM a high density, high speed, and low power, general purpose memory prompted the Defense Advanced Research Projects Agency to fund three MRAM consortia beginning in 1995, led by IBM, Motorola, and Honeywell, respectively. Other companies engaged in MRAM research are Hewlett-Packard, Matsushita, NEC, Fujitsu, Toshiba, Hitachi, and Siemens.

The key for a competitive MRAM technology is the fabrication of deep submicron-dimension magnetic cells. The further development of lithography tools utilizing e-beam and deep ultraviolet radiation is essential. Magnetic storage elements as small as $0.25\text{ }\mu\text{m}$ have been demonstrated by both Motorola and IBM (Tehrani et al. 1996; Chen et al. 1997; Gallagher et al. 1997). Among the steps of MRAM fabrication that are not yet compatible with semiconductor processing is the ion milling of the magnetic cells. The possibility of dry etching the magnetic materials has, nevertheless, been demonstrated (Jung et al. 1997). Figures 5.12 through 5.15 summarize the major directions in memory R&D. Arrows denote ferromagnetic layers.

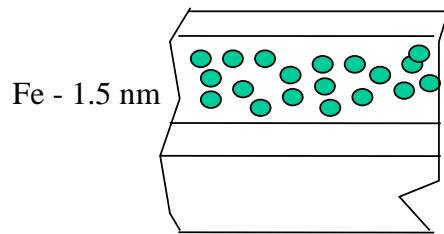


Figure 5.12. Granular GMR—Co, Fe (Nagoya University, Tohoku University, CNRS-Thomson, UCSB, UCSD).

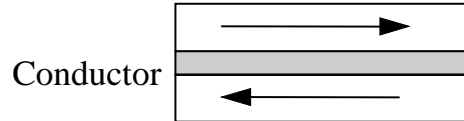


Figure 5.13. Current in plane (Matsushita, Fujitsu, Mitsubishi, Toshiba, Hitachi, Thomson, Philips, Siemens, IBM, Univ. Regensburg, IMEC, Nagoya University, Tohoku University, NIST).

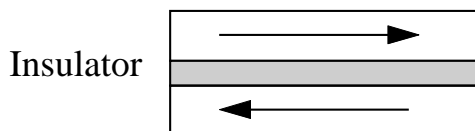


Figure 5.14. Magnetic tunnel junction (IBM, MIT, HP, Tohoku University).

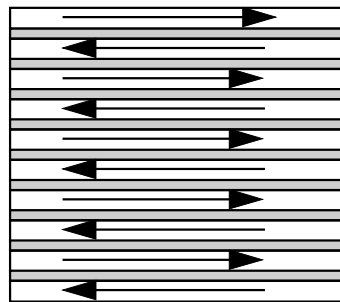


Figure 5.15. Ferromagnetic/metal/ferromagnetic: 3 - 60 periods free-standing (NRL, CNRS-Thomson, Philips, Michigan State, Lawrence Livermore Labs); plated into pores (L'École Polytechnique Fédérale de Lausanne, Johns Hopkins University, Université Catholique Louven).

The ability to fabricate submicron magnetic elements has opened a very rich and fascinating area of micromagnetics research. Characterization techniques having nanoscale resolution have been utilized and improved to measure and image the complex magnetization patterns in order to understand the magnetization switching characteristics. Examples of such techniques include the following:

- superconducting quantum interference device (SQUID) magnetometry (Zhu et al. 1997)
- magnetic force microscopy (MFM) (Ohkubo et al. 1991)
- scanning electron microscopy with polarization analysis (SEMPA) (Scheinfein et al. 1990)
- magnetic near-field microscopy (Betzig and Trautmann 1992)
- electron holography (Mankos et al. 1995)

Another essential tool is micromagnetics modeling, which is used to predict complex magnetic domain configurations in patterned magnetic elements and to generate transient pictures that demonstrate the process of forming complex domain configurations (Zheng and Zhu 1997).

By combining MFM, SQUID magnetometry, SEMPA, and micromagnetics modeling, researchers at Motorola have conducted a systematic study of the switching characteristics of single-layer and multilayer submicron magnetic structures. Three different phases of the magnetization phase diagram have been identified with regards to material composition, dimension, shape, thickness, and other structural parameters: (1) the quasi-single domain phase can be well described by the coherent rotation model (Sakaki et al. 1995); (2) the end-domain phase is dominated by the nonuniform regions of magnetization at the two ends of the element—the magnetization switching process can either be rotational or through domain wall nucleation and propagation (Shi et al. 1998); and (3) the trapped magnetization vortice (TMV) phase, which is characterized by the presence

of magnetization vortices. Nucleation from TMV sites requires lower reversal fields than coherent rotation, but a high field is needed to drive out TMVs in the element. When the driving field is not high enough, TMVs can cause unusually large fluctuations in the switching field (Shi et al. n.d.).

As the size of magnetic elements scales below 20 nm, a superparamagnetic phase emerges in which the room temperature thermal energy overcomes the magnetostatic energy well of the element, resulting in zero hysteresis (Hylton 1993). In other words, although the element itself is a single-domain ferromagnet, the ability of an individual magnetic “dot” to store magnetization orientation information is lost when its dimension is below a threshold. On the other hand, suitably prepared alloys of immiscible ferromagnetic and nonmagnetic metals that contain single-domain ferromagnetic grains in a nonmagnetic matrix have been shown to exhibit GMR characteristics. The moments of the magnetic grains are aligned at high fields and random at the coercive field, leading to GMR characteristics. In such “granular” metals, GMR has been reported for sputtered alloy films of CoCu (Berkowitz et al. 1992; Xiao et al. 1992), FeCu (Xiao et al. 1992), NiFe/Ag (Jiang et al. 1992), and CoAg (Carey et al. 1992; Tsoukatos et al. 1992). GMR values as high as 55% at 4.2 K and 20% at room temperature have been observed. The granular films require magnetic fields of the order of 10 kOe to achieve such a change in electrical resistance.

A very exciting consequence of ultrascaled magnetic particles is quantum tunneling of the magnetization direction of a collection of spins. There is no simple Schrödinger equation that describes this process, since it is not an elementary particle that is tunneling but a collective coordinate. Below its “blocking temperature,” at which thermally assisted hopping between magnetic orientations becomes frozen out, magnetic particles of TbCeFe at sizes around 15 nm have been observed to behave independent of temperature and with no freeze-out magnetic relaxation (Barbara et al. 1993). Because of the coherent tunneling of the magnetization orientation between the symmetric double-well potential, a resonance line in the magnetic susceptibility and noise spectra has been observed at temperatures below 200 mK in zero applied magnetic field (Awschalom et al. 1992). This work has stimulated a number of theoretical investigations into the effects of dissipation and the feasibility of producing quantum effects in larger magnetic structures (Prokofev and Stamp 1993; Gaarg 1994; Braun and Loss 1994).

Another interesting type of nanomagnetic structure is nanometer ferromagnetic wires fabricated using conventional nanolithography (Adeyeye et al. 1997; Chou 1997), nanoimprint lithography (Chou et al. 1995), AFM/MFM direct writing (Kong et al. 1997), groove deposition (Hong and Giordano 1995), and electrodeposition into pores of template polymer membranes (Piraux et al. 1994; Blondel et al. 1994). Such nanowires of either single layer or multilayers may provide new approaches

to very small magnetoresistive sensors, ultrahigh-density hard disks (Chou et al. 1994), and other extensions of conventional applications. Another intriguing possibility is the suggestion to use heterostructure nanowires to investigate single electron tunneling (Cavicchi and Silsbee 1984; Kumzerov and Poborchii 1994).

Recently, molecular magnetism has received much attention with the development of a variety of synthesis techniques largely adapted from biology and chemistry (Kahn 1993). Natural and artificial ferritin proteins are examples of systems obtained using these methods (Gatteschi et al. 1994). The ability to add one magnetic ion at a time has resulted in nanoscale magnets precisely defined by atomic weight. Ferritin consists of a segmented protein shell in the shape of a hollow sphere, with an outer diameter of 12.5 nm and an inner diameter of 7.5 nm. *In vivo*, the inner space is normally filled with a crystal of an iron oxide that is antiferromagnetic below 240 K. The empty protein shells can also serve as vessels for the synthesis of ferrimagnetic magnetite and maghemite. Thus, there exists a system in which its size as well as the nature of its magnetic interactions can be varied.

Another example of molecular magnetism is a cobalt-iron-cyanide-based Prussian blue analog (Sato et al. 1996a). In the ground state the Fe^{+2} and Co^{+3} ions are low-spin and diamagnetic, and there is no interaction between them. Red light excitation transfers one electron from an iron site to a cobalt site, resulting in high-spin Fe^{+3} and Co^{+2} ions and magnetic interactions between them. The application of a blue light causes a transition back to the initial state and switches off the $\text{Fe}^{+3}\text{-Co}^{+2}$ interactions. In addition to this kind of photochemically controllable magnets, electrochemically controllable magnets have also been reported (Sato et al. 1996b).

QUANTUM DOT LASERS

Semiconductor lasers are key components in a host of widely used technological products, including compact disk players and laser printers, and they will play critical roles in optical communication schemes. The basis of laser operation depends on the creation of nonequilibrium populations of electrons and holes, and coupling of electrons and holes to an optical field, which will stimulate radiative emission. Calculations carried out in the early 1970s by C. Henry (Dingle and Henry 1976) predicted the advantages of using quantum wells as the active layer in such lasers: the carrier confinement and nature of the electronic density of states should result in more efficient devices operating at lower threshold currents than lasers with “bulk” active layers. In addition, the use of a quantum well, with discrete transition energy levels dependent on the quantum well dimensions

(thickness), provides a means of “tuning” the resulting wavelength of the material. The critical feature size—in this case, the thickness of the quantum well—depends on the desired spacing between energy levels. For energy levels of greater than a few tens of millielectron volts (meV, to be compared with room temperature thermal energy of 25 meV), the critical dimension is approximately a few hundred angstroms. Although the first quantum well laser, demonstrated in 1975, was many times less efficient than a conventional laser (van der Ziel et al. 1975), the situation was reversed by 1981 through the use of new materials growth capabilities (molecular beam epitaxy), and optimization of the heterostructure laser design (Tsang 1982).

Even greater benefits have been predicted for lasers with quantum dot active layers. Arakawa and Sakaki (1982) predicted in the early 1980s that quantum dot lasers should exhibit performance that is less temperature-dependent than existing semiconductor lasers, and that will in particular not degrade at elevated temperatures. Other benefits of quantum dot active layers include further reduction in threshold currents and an increase in differential gain—that is, more efficient laser operation (Asada et al. 1986). Figures 5.16 and 5.17 illustrate some of the key concepts in the laser operation. Stimulated recombination of electron-hole pairs takes place in the GaAs quantum well region, where the confinement of carriers and of the optical mode enhance the interaction between carriers and radiation (Fig. 5.16). In particular, note the change in the electronic density of states, as a function of the “dimensionality” of the active layer, shown in Figure 5.17. The population inversion (creation of electrons and holes) necessary for lasing occurs more efficiently as the active layer material is scaled down from bulk (3-dimensional) to quantum dots (0-dimensional). However, the advantages in operation depend not only on the absolute size of the nanostructures in the active region, but also on the uniformity of size. A broad distribution of sizes “smears” the density of states, producing behavior similar to that of bulk material.

Thus, the challenge in realizing quantum dot lasers with operation superior to that shown by quantum well lasers is that of forming high quality, uniform quantum dots in the active layer. Initially, the most widely followed approach to forming quantum dots was through electron beam lithography of suitably small featured patterns ($\sim 300 \text{ \AA}$) and subsequent dry-etch transfer of dots into the substrate material. The problem that plagued these quantum dot arrays was their exceedingly low optical efficiency: high surface-to-volume ratios of these nanostructures and associated high surface recombination rates, together with damage introduced during the fabrication itself, precluded the successful formation of a quantum dot laser.

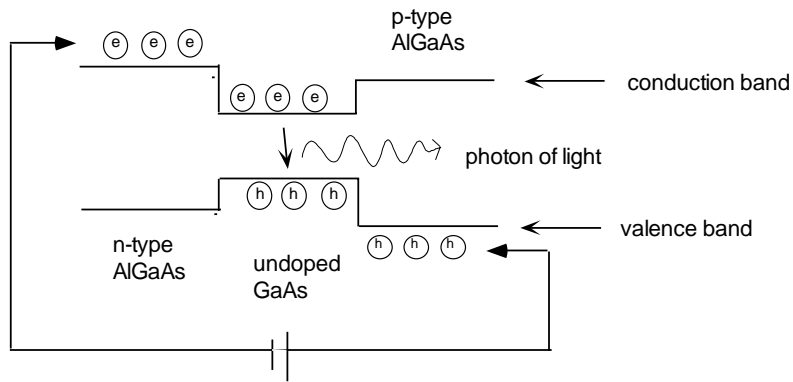


Figure 5.16. Schematic of a semiconductor laser.

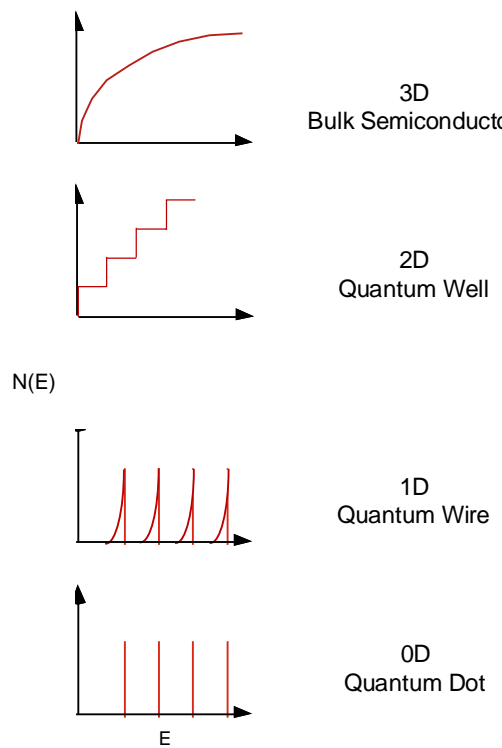


Figure 5.17. Density of electronic states as a function of structure size.

With the demonstration of the high optical efficiency self-assembled formation of quantum dots (see Chapter 2), formed without need of external processing and having the natural overgrowth of cladding material (which addressed issues of surface recombination), there ensued a marked increase

in quantum dot laser research. The first demonstration of a quantum dot laser with high threshold density was reported by Ledentsov and colleagues in 1994. Bimberg et al. (1996) achieved improved operation by increasing the density of the quantum dot structures, stacking successive, strain-aligned rows of quantum dots and therefore achieving vertical as well as lateral coupling of the quantum dots. In addition to utilizing their quantum size effects in edge-emitting lasers, self-assembled quantum dots have also been incorporated within vertical cavity surface-emitting lasers. Table 5.4 gives a partial summary of the work and achievements in quantum dot lasers.

As with the demonstration of the advantages of the quantum well laser that preceded it, the full promise of the quantum dot laser must await advances in the understanding of the materials growth and optimization of the laser structure. Although the self-assembled dots have provided an enormous stimulus to work in this field, there remain a number of critical issues involving their growth and formation: greater uniformity of size, controllable achievement of higher quantum dot density, and closer dot-to-dot interaction range will further improve laser performance. Better understanding of carrier confinement dynamics and capture times, and better evaluation of loss mechanisms, will further improve device characteristics. It should be noted that the spatial localization of carriers brought about by the quantum dot confinement may play a role in the “anomalous” optical efficiency of the GaN-based materials, which is exceptional in light of the high concentration of threading dislocations ($\sim 10^8 - 10^{10} \text{ cm}^{-2}$) that currently plague this material system. The localization imposed by the perhaps natural nanostructure of the GaN materials may make the dislocation largely irrelevant to the purely optical (but not to the electrical) behavior of the material.

CARBON NANOTUBES

The first synthesis and characterization of carbon nanotubes were reported by Iijima from NEC in late 1991. The initial theoretical study of their electronic structure was soon followed with the work by Dresselhaus and coworkers at MIT (Dresselhaus et al. 1992; Saito et al. 1992a; Saito et al. 1992b). Since then, the fabrication of nanotubes has been improved by several groups, and methods other than arc discharge have been explored. The main issues are to separate the nanotubes from other forms of carbon also produced in the fabrication process and to increase the yield of single-walled nanotubes (SWNT) for potential applications. Following Iijima’s work, macroscopic quantities of MWNT were produced with an improved arc discharge method by Ebbesen and coworkers at NEC (Tsukuba) (Ebbesen and Ajayan 1992).

TABLE 5.4. Summary of Quantum Dot Laser Results

Year	QD composition & size	Threshold (kA/cm ²)	Operating T (K)	Wavelength (μm)	Reference
1994	InAs 7 nm	1 0.1	300 77	0.9 0.95	(Kirstaedter et al. 1994) Europe/Russia
1994	InGaAs 30 nm	7.6	77	1.26	(Hirayama et al. 1994) Japan
1995	In _{0.5} Ga _{0.5} As 20 nm	0.8	85	0.92	(Shoji et al. 1995) Japan
1996	InP 25 nm	25	300	0.7	(Moritz et al. 1996) Europe
1996	In _{0.3} Ga _{0.7} As	0.5 1.2	300	1.2 1	(Miran et al. 1996) United States
1996	In _{0.4} Ga _{0.6} As 12 nm	0.65	300	1	(Kamath et al. 1996) United States
1996	In _{0.5} Ga _{0.5} As 10 layers	0.06	300	1	(Ledentsov et al. 1996) Russia/Europe

Source: Bimberg et al. 1997

It was not until 1995 that Smalley and colleagues at Rice University showed that SWNT can be efficiently produced by laser ablation of a graphite rod (Guo et al. 1995). In the following year, that same group produced what is considered to be among the best SWNT material generated so far; over 70% of the volume of material was nanotubes bundled together into crystalline ropes of metallic character (Thess et al. 1996). Also in 1996, a group from the Chinese Academy of Science used chemical vapor deposition to produce a 50 mm thick film of nanotubes that were highly aligned perpendicular to the surface (Li et al. 1996). Progress in recent years leads one to predict that it will indeed be possible to produce high quality carbon nanotubes in macroscopic quantities needed for many of the applications outlined below.

Nanotube bundles form a low density material and are expected to have high stiffness and axial strength as a result of their seamless cylindrical graphitic structure. It is therefore predicted that they can be used to fabricate a material with better mechanical properties than the present carbon fiber materials. Information about the mechanical properties of nanotubes has been gathered recently by a study of the thermal vibrations of a single

SWNT attached to a substrate (Treacy et al. 1996). Ebbesen's group at the Princeton NEC Research Institute found that nanotubes have an exceptionally high Young's modulus ($\sim 2 \times 10^9$ Pa) (Treacy et al. 1996). In order to reach a better understanding of the mechanical properties and intrinsic limitations of nanotubes, Bernholc's group from North Carolina State University theoretically studied the behavior of nanotubes beyond the linear Hooke's law and the nature of the defects leading to dislocations and fractures (Yakobson et al. 1996; Nardelli et al. 1998).

Nanotubes are highly polarizable nanoscale straws, a property that confers on them the capacity to ingest inorganic elements by nanocapillarity (Pederson and Broughton 1992). As a result, it has been conjectured that they could be used as minute molds to shape nanometer-sized quantum wires and as miniature test tubes. Ajayan and coworkers at NEC (Tsukuba) have first shown that lead can be introduced into carbon nanotubes (Ajayan and Iijima 1993). The efficiency of their process is low, and prior removal of the caps from the ends of the nanotubes is expected to improve the situation (Tsang et al. 1993). More information about the mechanism of NT filling was obtained by Pascard and coworkers from the École Polytechnique in France by studying the propensity to form nanowires for 15 encapsulated metal elements (Guerret-Plécourt et al. 1994). Finally, external decoration of nanotubes with metal atoms has been demonstrated and is predicted to have applications in catalysis (Satishkumar et al. 1996). Table 5.5 summarizes the primary methods of nanotube fabrication and the institutions engaged in specific methods of nanotube fabrication.

Early theoretical studies already showed that the electronic properties of nanotubes strongly depend on their diameter and their chirality leading to metallic or semiconducting structures (Saito et al. 1992c). It was conjectured that these properties can be used to construct nanoscale electronic devices. While theoretical studies were promptly published, it was only in 1996 that Ebbesen and coworkers (1996) at the Princeton NEC Research Institute presented reliable four-point probe conductivity measurements on MWNT, confirming the theoretical predictions. In 1997, two groups, one at Lawrence Berkeley National Laboratory (Bockrath et al. 1997) and the second at Delft University (Tans et al. 1997) in the Netherlands showed that conductivity through nanotubes is controlled by low dimensional effects such as resonant tunneling and single-electron charging effects. Hall effect measurements at the École Polytechnique Fédérale de Lausanne (EPFL) in Switzerland have shown that hole transport is predominant in electronic conductance (Baumgartner et al. 1997). Despite these and other very recent and encouraging efforts such as those studying the mean free path of carriers in nanotubes, the conduction mechanism is still only partially understood (Petit et al. 1997).

TABLE 5.5. Nanotube Fabrication Methods

Method	Institution
Laser ablation – SWNT	Rice University
Arc discharge – SWNT	University of Montpellier
	University of Kentucky
Arc discharge - MWNT	NEC
Chemical vapor deposition - aligned MWNT	Beijing

Metallic nanotubes are strongly polarizable in an electric field and thereby lead to field enhancement at their extremity, the strength of which depends on the ratio of the diameter to the length and can be extremely large for routinely produced nanotubes. For this reason and possibly others related to quantum confinement effects, nanotubes are expected to form outstanding field-emitting materials. In 1995, the Rice University group showed that nanotubes emit electrons very efficiently when immersed in an electric field and irradiated by a laser to remove their cap (Rinzler et al. 1995). They attribute their observation to the unraveling of an atomic wire of carbon atoms. Efficient field emission was also obtained from carefully aligned nanotubes by de Heer and coworkers (1995) at EPFL, whereas Collins and coworkers from the University of California at Berkeley (Collins and Zettl 1996, 1997), have used randomly oriented nanotubes with similar results. Efficient field-emitting material is highly desirable for the production of field-emission displays and microwave tubes.

Recently, a group from Mie University in Japan has built a cathode ray tube (CRT) using nanotube field emitters (Saito et al. n.d.). In this work, the layers of nanotubes were cut out from the soot produced in an arc discharge chamber. This fabrication method is presently not compatible with industrial production requirements, and more progress must be made before this effort can be translated into an industrial product. Table 5.6 summarizes the electrical and field emission properties of nanotubes, with the representative institutions pursuing these studies.

In summary, macroscopic amounts of good quality nanotubes can presently be fabricated by several groups around the world, and the theoretical understanding of the electronic structure and related properties of nanotubes has reached a very good level. However, despite the fact that many potential applications are mentioned in the literature over and over again, only the outstanding field emission properties of nanotubes have achieved realization in practical devices. One of the main obstacles simply remains the controlled manipulation of nanoscale objects. In this respect it seems that the generation of self-aligned structures is a path to explore further, especially after the encouraging successes reported in the literature in 1997-98.

TABLE 5.6. Electrical and Field Emission Properties of Nanotubes

Results	Institution
Theory and experiment: nanotubes can be metallic or semiconducting	MIT, NEC
Conductivity shows low dimensional signature	LBNL
Field emission from unraveled carbon chains at the end of nanotubes	Delft University
Field emission from aligned nanotubes attached to scanning probe tip	Rice University
CRTs fabricated with nanotubes as field emitters	EPFL
	Mie University

REFERENCES

- Adeyeye, A., G. Lauhoff, J. Bland, C. Daboo, D. Hasko, and H. Ahmed. 1997. *Appl. Phys. Lett.* 70:1046.
- Ajayan, P.M., and S. Iijima. 1993. *Nature*. 361:333.
- Arakawa, Y., H. Sakaki. 1982. *Appl. Phys. Lett.* 40: 939.
- Asada, M., Y. Mayamoto, and Y. Suematsu. 1986. *IEEE Journ. Quantum Electronics* QE-22(9): 1915-1921.
- Averin, D.V., and K.K. Likharev. 1991. Chapter 6 in *Mesoscopic phenomena in solids*, ed. B.L. Altshuler, P.A. Lee, and R.A. Webb. Amsterdam: Elsevier.
- Awschalom, D., D. DiVincenzo, and J. Smyth. 1992. *Science* 258:414.
- Baibich, M.N., J.M. Broto, A. Fert, F. Nguyen Van Dau, F. Petroff, P. Etienne, G. Creuzet, A. Friederich, and J. Chazelas. 1988. *Phys. Rev. Lett.* 61:2472.
- Barbara, B., L.C. Sampaio, J.E. Wegrowe, B.A. Ratnam, A. Marchand, C. Paulsen, M.A. Novak, J.L. Tholence, M. Uehara, and D. Fruchart. 1993. *J. Appl. Phys.* 73:6703.
- Barker, J. R., S. Roy, S. Babiker, and A. Asenov. 1997. *Proceedings of the International Conference on Quantum Devices and Circuits*. Singapore: World Scientific.
- Baumgartner, G., M. Carrard, L. Zuppiroli, W. Bacsa, W.A. de Heer, and L. Forró. 1997. *Phys. Rev. B*. 55:6704.
- Berkowitz, A.E., J.R. Mitchell, M.J. Carey, A.P. Young, S. Zhang, F.E. Spada, F.T. Parker, A. Hutten, and G. Thomas. 1992. *Phys. Rev. Lett.* 68:3745.
- Betzig, E., and J. Trautmann. 1992. *Science* 257:189.
- Bimberg, D., N. Ledentsov, M. Grundmann, N. Kirstaedter, O. Schmidt, M. Mao, V. Ustinov, A. Egorov, P. Kop'ev, Zh. Alferov, S. Ruvimov, U. Gösele, and J. Heydenreich. 1996. *Jap. Journal. Appl. Phys.* 35 1311-1219.
- Bimberg, D., N. Kirstaedter, N.N. Ledentsov, Zh. Alferov, P.S. Kop'ev, and V.M. Ustinov. 1997. *IEEE Selected Topics in Quantum Electronics* 3:196-205.
- Blondel, A., J. Meier, B. Doudin, and J. Ansermet. 1994. *Appl. Phys. Lett.* 65:3019.
- Bockrath, M., D.H. Cobden, P.L. McEuen, N.G. Chopra, A. Zettl, A. Thess, and R.E. Smalley. 1997. *Science* 275:1922.
- Braun, H., and D. Loss. 1994. *J. Appl. Phys.* 73:6177.
- Nardelli, M.B., B.I. Yakobson, and J. Bernholc. 1998. *Phys. Rev. B* 57:R4277.
- Carey, M.J., A.P. Young, A. Starr, D. Rao, A.E. Berkowitz, and J.S. Jiang. 1992. *Appl. Phys. Lett.* 61:2935.

- Carlsson, S.-B., T. Junno, H. Xu, L. Montelius, and L. Samelson. 1997. *Extended abstracts of the 3rd International Workshop on Quantum Functional Devices*. Tokyo: R&D Association for FED.
- Cavicchi, R., and R. Silsbee. 1984. *Phys. Rev. Lett.* 52:1453.
- Chen, E., S. Tehrani, T. Zhu, M. Durlam, and H. Goronkin. 1997. *J. Appl. Phys.* 81:3992.
- Chou, S. 1997. *Proceedings of the IEEE* 85:652.
- Chou, S., P. Krauss, and P.R. Enstrom. 1995. *Science* 272:8.
- Chou, S., M. Wei, P. Krauss, and P. Fischer. 1994. *J. Appl. Phys.* 76:6673.
- Collins, P., and A. Zettl. 1996. *Appl. Phys. Lett.* 69:1969.
- Collins, P., and A. Zettl. 1997. *Phys. Rev. B.* 55:9391.
- de Heer, W.A., A. Chatelain, and D. Ugarte. 1995. *Science* 270:1179.
- Dingle, R., and C.H. Henry. 1976. Quantum effects in heterostructure lasers. U.S. Patent 3982207 (Sept. 21).
- Dieny, B., V.S. Speriosu, B.A. Gurney, S.S.P. Parkin, D.R. Wilhoit, K.P. Roche, S. Metin, D.T. Peterson, and S. Nadimi. 1991a. *J. Mag. Magn. Mater.* 93:101.
- Dieny, B., V.S. Speriosu, S. Metin, S.S.P. Parkin, B.A. Gurney, P. Baumgart, and D.R. Wilhoit. 1991b. *J. Appl. Phys.* 69:4774.
- Dresselhaus, M.S., G. Dresselhaus, and R. Saito. 1992. *Phys. Rev. B.* 45:6234.
- Ebbesen, T.W., and P.M. Ajayan. 1992. *Nature* 358: 220.
- Ebbesen, T. W., H. J. Lezec, H. Hiura, J. W. Bennett, H. F. Ghaemi, and T. Thio. 1996. *Nature*. 382:54.
- Eberl, K., P.M. Petroff, and P. Demmester, eds. 1995. *Low dimensional structures prepared by epitaxial growth or regrowth on patterned substrates*. Dordrecht: Kluwer.
- Futatsugi, T., Y. Awano, Y. Sakuma, M. Shima, Y. Sugiyama, H. Nakao, T. Strutz, M. Takatsu, and N. Yokoyama. 1997. *Extended abstracts of the 16th Symposium on Future Electron Devices*. Tokyo: R&D Association for FED.
- Gaarg, A. 1994. *J. Appl. Phys.* 76:6168.
- Gallagher, W.J., S.S.P. Parkin, X. Bian, A. Marley, K. Roche, R. Altman, S. Rishton, C. Jahnes, T. Shaw, and G. Xiao. 1997. *J. Appl. Phys.* 81:3741.
- Gatteschi, D., A. Caneschi, L. Paedi, and R. Sessoli. 1994. *Science* 265:1054.
- Guerret-Plécourt, C., Y. Le Bouar, A. Loiseau, and H. Pascard. 1994. *Nature* 372:76.
- Guo, L., E. Leobandung, and S.Y. Chou. 1977. *Science* 275:649.
- Guo, T., P. Nikolaev, A. Thess, D.T. Colbert, and R.E. Smalley. 1995. *Chem. Phys. Lett.* 243:49.
- Hirayama, H., K. Matsunaga, M. Asada, and Y. Suematsu. 1994. *Electronics Letters* 30:142-3.
- Hong, K., and N. Giordano. 1995. *J. Mag. Magn. Mater.* 151:396.
- Hylton, T. 1993. *Appl. Phys. Lett.* 62:2431.
- Iijima, S. 1991. *Nature* 354:56.
- Jiang, J.S., J.Q. Xiao, and C.L. Chien. 1992. *Appl. Phys. Lett.* 61:362.
- Jung, K., J. Shi, K. Nordquist, S. Tehrani, M. Durlam, E. Chen, and H. Goronkin. 1997. *IEEE Trans. Mag.* 33:3601.
- Kahn, O. 1993. In *Molecular magnetism*. New York: VCH.
- Kamath, K., P. Bhattacharya, T. Sosnowski, T. Norris, and J. Phillips. 1996. *Electronics Letters* 32:1374-75.
- Kirstaedter, N., N. Ledentsov, M. Grundmann, D. Bimberg, V. Ustinov, S. Ruvimov, M. Maximov, P. Kop'ev, and Zh. Alferov. 1994. *Electronics Letters* 30:1416-7.
- Koga, J.K., K. Uchida, and A. Toriumi. 1997. *Extended abstracts of the 16th Symposium on Future Electron Devices*. Tokyo: R&D Association for FED.
- Kong, L., L. Zhuang, and S. Chou. 1997. *IEEE Trans. Mag.* 33:3019.
- Kumzerov, Y., and V. Poborchii. 1994. *Phantoms* 4:2.
- Ledentsov, N.N., M. Grundmann, N. Kirstaedter, J. Christen, R. Heitz, J. Börher, F. Heinrichsdorff, D. Bimberg, S.S. Ruvimov, P. Werner, U. Richter, U. Gösele, J.

- Heydenreich, V.M. Ustinov, A.Yu. Egorov, M.V. Maximov, P.S. Kop'ev, and Zh.I. Alferov. 1994. *Proc. ICPS-22*, Vancouver 3:1855. Singapore: World Scientific.
- Ledentsov, N.N., V.A. Shchukin, M. Grundmann, N. Kirstaedter, J. Börher, O.G. Schmidt, D. Bimberg, V.M. Ustinov, A. Yu. Egorov, A.E. Zhukov, P.S. Kop'ev, S.V. Zaitsev, N.Yu. Gordeev, and Zh.I. Alferov. 1996. *Physical Review B* 54:8743-50.
- Lent, C.S., P.D. Tougaw, W. Porod, and G.H. Bernstein. 1993. *Nanotechnology* 4:49.
- Li, W.Z., S.S. Xie, L.X. Qian, B.H. Chang, B.S. Zou, W.Y. Zhou, R.A. Zhao, and G. Wang. 1996. *Science* 274:1701.
- Likharev, K.K. 1998. *IBM J. Res. Dev.* 32:144.
- Mankos, M., P. de Haan, V. Kambersky, G. Matteucci, M. McCartney, Z. Yang, M. Scheinfein, and J. Cowley. 1995. In *Electron holography*, ed. A. Tonomura. Elsevier.
- Mirin, R., A. Gossard, and J. Bowers. 1996. *Proceedings, Int. Conf. Quantum Devices and Circuits*, ed. K. Ismail, S. Bandyopadhyay, and J.P. Leburton. Singapore: World Scientific.
- Miyazaki, T., and N. Tezuka. 1995. *J. Mag. Magn. Mater.* 139:L231.
- Moodera, J.S., L.R. Kinder, T.M. Wong, and R. Merservey. 1995. *Phys. Rev. Lett.* 74:3273.
- Moritz, A, R. Wirth, A. Hangleiter, A. Kurtenback, and K. Eberl. 1996. *Appl. Phys. Lett.* 69:212-214.
- Nakajima, A., T. Futatsugi, K. Kosemura, T. Fukano, and N. Yokoyama. 1997. *Appl. Phys. Lett.* 70:1742.
- Nakazato, K. 1996. *Extended abstracts of 15th Symposium on Future Electron Devices*. Tokyo: R&D Association for FED.
- Nakazato, K., T. J. Thornton, J. White, and H. Ahmed. 1992. *Appl. Phys. Lett.* 61:3145.
- Nötzel, R. 1996. *Semicond. Sci. Technol.* 11:1365, and references therein.
- Ohata, A., and A. Toriumi. 1996. *IEICE Trans. Electron.* E79-C:1586.
- Ohkubo, T., J. Kishigami, K. Yanagisawa, and R. Kaneko. 1991. *IEEE Trans. Magn.* 6:5286.
- Parkin, S.S.P., N. More, and K.P. Roche. 1990. *Phys. Rev. Lett.* 64:2304.
- Pederson, M.R. and J.Q. Broughton. 1992. *Phys. Rev. Lett.* 69:2689.
- Petit, P., E. Jouguelet, J.E. Fischer, A.G. Rinzler, and R.E. Smalley. 1997. *Phys. Rev. B* 56:9275.
- Petroff and Demmester. 1995. In *Low dimensional structures*, ed. Eberl et al.
- Piraux, L., J. George, J. Despres, C. Leroy, E. Ferain, R. Legres, K. Ounadjela, and A. Fert. 1994. *Appl. Phys. Lett.* 65:2484.
- Prokofev, N., and P. Stamp. 1993. *J. Phys. Condensed Mater.* 5:L663.
- Reed, M.A., C. Zhou, C.J. Muller, T.P. Burgin, and J. M. Tour. 1997. *Science* 278:252.
- Rinzler, A.G., J.H. Hafner, P. Nikolaev, L. Lou, S.G. Kim, D. Tománek, P. Nordlander, D.T. Colbert, and R.E. Smalley. 1995. *Science* 269:1550.
- Roychowdhury, V.P., D.B. Janes, S. Bandyopadhyay, and X. Wang. 1966. *IEEE Trans. Electron Devices* 43:1688.
- Saito, R., G. Dresselhaus, and M.S. Dresselhaus. 1992a. *Appl. Phys. Lett.* 60:2204.
- Saito, R., M. Fujita, G. Dresselhaus, and M.S. Dresselhaus. 1992b. *Phys. Rev. B* 46:1804.
- _____. 1992c. *Appl. Phys. Lett.* 60:2204.
- Saito, Y., S. Uemura, and K. Hamaguchi. 1998. *Jap. J. Appl. Phys.* 37:L346.
- Sakaki, H., G. Yusa, T. Someya, Y. Ohno, T. Noda, H. Akiyama, Y. Kadoya, and H. Noge. 1995. *Appl. Phys. Lett.* 67:3444.
- Satishkumar, B.C., E.M. Vogl, A. Govindaraj, and C.N.R. Rao. 1996. *J. Phys. D* 29:3173.
- Sato, O., T. Iyoda, A. Fujishima, and K. Hashimoto. 1996a. *Science* 272:704.
- Sato, O., T. Iyoda, A. Fujishima, and K. Hashimoto. 1996b. *Science* 271:49.
- Scheinfein, M., J. Unguris, M. Kelley, D. Pierce, and R. Celotta. 1990. *Rev. Sci. Instrum.* 61:2501.
- Shi, J., T. Zhu, M. Durlam, E. Chen, and S. Tehrani. 1998. *J. Appl. Phys.* (In press.)
- Shi, J., T. Zhu, S. Tehrani, Y. Zheng, and J.G. Zhu. N.d. submitted to *Phys. Rev. Lett.*

- Shinjo, T. and T. Takada. 1987. Metallic superlattices. In *Ferromagnetic Materials*, Vol. 3, ed. E.P. Wohlfarth.4 Amsterdam: Elsevier.
- Shoji, H., K. Mukai, N. Ohtsuka, M. Sugawara, T. Uchida, and H. Ishikawa. 1995. *IEEE Photonic Technology Letters* 7:1385-87.
- Snider, G.L., A.O. Orlov, I. Amlani, G.H. Bernstein, C.S. Lent, J.L. Merz, and W. Porod. 1997. *Extended abstracts of the 3rd International Workshop on Quantum Functional Devices*. Tokyo: R&D Association for FED.
- Taira, K., T. Suzuki, H. Ono, K. Nomoto, and I. Hase. 1997. *Extended abstracts of the 3rd International Workshop on Quantum Functional Devices*. Tokyo: R&D Assn. for FED.
- Tans, S.F., M.H. Devoret, H. Dai, A. Thess, R.E. Smalley, L.J. Geerligs, and C. Dekker. 1997. *Nature* 386:474.
- Tehrani, S., E. Chen, M. Durlam, T. Zhu, and H. Goronkin. 1996. *IEDM Digest* 96:193.
- Thess, A., R. Lee, P. Nikolaev, H. Dai, P. Petit, J. Robert, C. Xu, Y.H. Lee, S.G. Kim, A.G. Rinzler, D.T. Colbert, G.E. Scuseria, D. Tománek, J.E. Fischer, and R.E. Smalley. 1996. *Science* 273:483.
- Tougaw, P.D., and C.S. Lent. 1994. *J. Appl. Phys.* 75:1818.
- Treacy, M.M.J., T.W. Ebbesen, and J.M. Gibson. 1996. *Nature* 38:678.
- Tsang, S.C., P.J.F. Harris, and M.L.H. Green. 1993. *Nature* 362:520.
- Tsang, W.T. 1982. *Appl. Phys. Lett.* 40:217-219.
- Tsukatos, A., H. Wan, G.C. Hadjipanayis, and Z.G. Li. 1992. *Appl. Phys. Lett.* 61:2059.
- Tsukagoshi, K., K. Nakazato, and T. Sato. 1997. *Extended abstracts of 16th Symposium on Future Electron Devices*. Tokyo: R&D Association for FED.
- van der Ziel, J.P., R. Dingle, R.C. Miller, W. Wiegmann, and W.A. Nordland, Jr. 1975. *Appl. Phys. Lett.* 26:463-465.
- Wesler, J.J., S. Tiwari, S. Rishton, K.Y. Lee, and Y. Lee. 1997. *IEEE Electron Rev. Lett.* 18:278.
- Woodham, R.G. and H. Ahmed. 1997. *Extended abstracts of the 3rd International Workshop on Quantum Functional Devices*. Tokyo: R&D Association for FED.
- Xiao, J.Q., J.S. Jiang, and C.L. Chien. 1992. *Phys. Rev. Lett.* 68:3749.
- Yakobson, B.I., C.J. Brabec, and J. Bernholc. 1996. *Phys. Rev. Lett.* 76:2511.
- Zheng, Y., and J.G. Zhu. 1997. *J. Appl. Phys.* 81:5471.
- Zhu, T., J. Shi, K. Nordquist, S. Tehrani, M. Durlam, E. Chen, and H. Goronkin. 1997. *IEEE Trans. Mag.* 33:3601.

